HAPTIC METAMERIC TEXTURES

Scinob Kuroki[1], Masataka Sawayama[1], and Shin'ya Nishida[1,2]

[1]NTT Communication Science Laboratories, NTT Corporation, Japan

[2]Departmen of intelligence science and technology, Graduate School of Informatics, Kyoto University

Abstract

The ability to recognize and discriminate complex surface textures through touch is essential to the survival of living beings, including humans. Most studies of tactile texture perception have emphasized perceptual impacts of lower-order statistical structures of stimulus surfaces that can be described in terms of amplitude spectra or spatial-frequency/orientation subband histograms (e.g., root mean squares of carving depth and inter-ridge distance). However, real-world surfaces we encounter in everyday life differ also in higher-order statistics that appear in phase spectra or joint subband histograms. Though human vision has sensitivity to higher-order statistics, and some studies have revealed similarities between visual and tactile information processing, it remains obscure whether human touch has sensitivity to higher-order statistics. Here we show that patterns different from each other in higher-order statistics, which can be easily distinguished by vision, cannot be distinguished by touch. We 3D-printed textured surfaces transcribed from different 'photos' of natural scenes such as stones and leaves. The textures look sufficiently different, and the maximum carving depth (2 mm) was well above the haptic detection threshold. Nevertheless, observers (n=10) could not accurately discriminate some texture pairs. Analysis of these stimuli showed that the more similar the amplitude spectrum was, the more difficult the discrimination became, suggesting a hypothesis that the high-order statistics have minor effects on tactile texture discrimination. We directly tested this hypothesis by matching the subband histogram of each texture using a texture synthesis algorithm. Haptic discrimination of these textures was found to be nearly impossible, although visual discrimination remained feasible due to differences in higher-order statistics. These findings suggest that human tactile texture perception qualitatively differs from visual texture perception with regard to insensitivity to higher-order statistical differences.

Significance

Humans sense spatial patterns in the surrounding world through their eyes and hands. Researchers have revealed a detailed hierarchical processing of image features for visual texture perception, while that for haptic texture perception remains obscure. One big bottleneck in tactile research has been difficulty in controlling stimulus patterns, but this issue is being resolved by recent technological progress. Here we move a step ahead by using a high-resolution 3D printer. We invented textured surfaces that were 3D-printed from visual images, and controlled low- and high-order statistics of the surfaces by changing features of the original images. Behavioural experiments showed that human observers have sensitivity to lower-order statistics, which is in line with previous studies, but we could not observe any positive evidence of sensitivity to higher-order statistics. Although recent studies have emphasized the similarity between touch to vision with regard to spatiotemporal processing, the present findings indicate a qualitative difference between the two modalities. That is, touch differs from vision not only in spatio-temporal resolution but also in (in)sensitivity to high-level image

statistics. Our findings support the view that the two modalities sense spatial information using different and complementary strategies.

Introduction

Most objects in the world are covered by surfaces with a variety of textures. By sensing surface textures, we, and many other animals, are able to specify distinct surface areas, identify materials, and estimate surface conditions. Vision and touch are the two main sensory modalities contributing to surface texture perception. Here we analyze tactile texture processing by referring to recent theories of visual texture perception.

Early studies on visual texture segregation revealed that the condition for two adjacent textures to be perceptually segregated is the presence of significant differences in the histogram of local orientation and spatial frequency (Gabor wavelets) (Julesz, 1962; Bergen & Adelson, 1988), which is presumably represented by the response distribution of V1 neurons. Recent studies examining the perceptual discrimination of natural textures further showed that two textures are perceptually indistinguishable (become a metameric pair) in peripheral vision when they are matched not only in terms of V1 image statistics, but also in terms of the joint statistics of V1 responses, to which V2 and the higher cortical areas are responsive (Freeman & Simoncelli, 2011; Freeman et al., 2013; Ziemba et al., 2016). Human observers can visually discriminate V2 metamer textures (with identical Gabor and joint statistics), but only when using elaborated attentive spatial processing by central vision (Freeman et al., 2013; Rosenholtz, 2016).

In this paper, we divide image statistics into two levels, with the boundary to separate the lower and higher orders being set between Gabor statistics (Julesz, 1962) (level #2 in Fig. 1) and joint statistics (Freeman & Simoncelli, 2011) (level #3 in Fig. 1). Approximately speaking, the former statistics is associated with the Fourie amplitude spectrum and with the second-order statistics in the terminology of Julesz (1962, see also Klein & Tyler, 1986; Hansen & Hess, 2006), while the latter statistics is associated with the phase spectrum. As noted above, visual texture perception is sensitive to higher-order statistics, in addition to lower-order statistics.

The somatosensory system has a spatial-information processing stream analogous to that of the visual system. First, a spatiotemporal pattern of skin deformation is sampled by mechanoreceptors. The signals from the mechanoreceptors are then pooled, suppressed by surrounds, and sent to the cortex via peripheral afferent neurons. Some peripheral afferents may be able to carry some orientation information (Delhaye et al., 2018; Pruszynski & Johansson, 2014), but orientation selectivity is much more common and robust in the primary somatosensory cortex (S1, area 3b) (e.g., Bensmaia et al., 2008). The tactile receptive field of S1 neurons can be approximated by Gabor functions (DiCarlo et al., 1998, 2000), as are the visual receptive field of V1 neurons. Somatosensory processing becomes

more elaborate beyond S1 (e.g., Thakur et al., 2006). For example, some neurons in S2 have selectivity for higher-order shape features, such as the curvature of line stimuli, similar to that of visual neurons in V4 (Yau et al., 2009).

Here we investigated the performance of the tactile system in discriminating a variety of texture patterns (artificial textures made of numerous Gabors, and visual natural textures). All the patterns were easy to discriminate by vision. Through the analysis of the tactile discrimination performance, we considered what sorts of texture differences the tactile system is sensitive to, and, more specifically, whether it can utilize higher-order image statistics (at or beyond level #3 in Fig. 1) as does visual texture perception. There is little psychophysical evidence that tactile texture discrimination is sensitive to higher-order image statistics. The major spatial property of tactile texture perception intensively investigated in the past is roughness (Bensmaia, 2009; Klatzky et al., 2013; Hollins et al., 1993, 2000; Tiest, 2010; Tiest and Kapers, 2006). (Other properties, such as hardness and stickiness, are not purely spatial.) The stimulus spatial parameters that are known to affect roughness, such as the spatial period and inter-ridge spacing (e.g. Goodwin et al., 1989; Lederman, 1983; Lederman et al., 1972; Sathian et al., 1989, Taylor and Lederman, 1975), can be described in terms of lower-order image statistics. However, the neural responses to shapes/curvatures (Yau et al., 2009, 2013) suggest potential sensitivity to joint statistics.

Most previous tactile texture studies used relatively simple artificial stimuli (e.g., dots, gratings (Bensmaia and Hollins, 2005; Goodwin et al., 1989; Hollins and Bensmaia, 2007; Lederman, 1983; Lederman and Taylor, 1972; Sathian et al., 1989, Taylor and Lederman, 1975)) or went with daily natural surfaces (e.g., fabric, wood, metal (Weber et al. 2013; Yokosaka et al. 2017)). With these stimuli, it is not easy to examine the contribution of higher-order image statistics separately from those of lower-order ones. Here we overcame this limitation using a high-resolution 3D printer. By carving the surface of a sample material with the printer, we transcribed complex visual patterns including natural image textures into patterns of surface depth modulation. By manipulating the image statistics of the printed patterns, we were able examined whether tactile texture perception can utilize higher-order texture statistics.

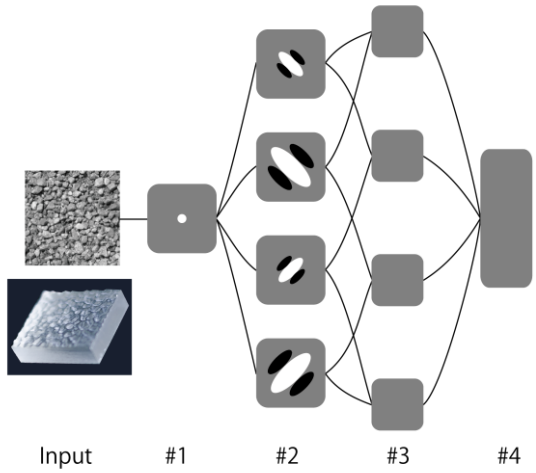

Fig. 1. Hypothetical diagram of hierarchical information processing in touch, inspired by visual processing.

Results

We evaluated human tactile accuracy in discriminating a pair of 3D-printed textures using an ABX task (Kingdom & Prins, 2010). After passively scanning three textures, A, B, and X in order, with the fingertip of the right index finger, the observer had to judge whether X was a 180°-rotated version of A or B (Fig. 2B). Since X was rotated, observers could not perform the task based on simple pattern matching. The maximum depth of the surface texture was approximately 2 mm, which was well above the minimum detectable depth magnitude (Bolanowski et al., 1988; Gescheider et al., 2001, 2002). Most previous studies on tactile texture perception asked observers to judge a specific roughness feature (e.g., "rate the roughness from 0 to 9" or "report which one was rougher"). In contrast, our method allowed us to account for any perceptual feature, including roughness, that the observers could use to discriminate stimuli. Furthermore, it enabled us to find two physically different textures that are 'metameric' (perceptually indiscriminable in any way).

In the first series of experiments, discrimination performance was measured for three sets of five textures (Fig. 2A). The first two sets were spatially bandpass random noise patterns, each made of numerous Gabor components. The variables across textures were the center frequency (CF) for the first set and the bandwidth (BW) for the second set. The last set consisted of five natural visual textures (hereafter referred to as natural scenes (NS)).

The discrimination performance of ten observers obtained with the CF-variable set was very good (Fig. 2C, top panel): a one-octave difference in the CF was sufficient for nearly perfect discrimination, except for the high-frequency pair (CF4 and CF5). The results are consistent with previous findings obtained with analogous conditions (e.g., Bensmaia, 2009; Klatzky et al., 2013; Tiest, 2010). Varying the BW, on the other hand, is a novel approach in the quest for haptic sensitive stimulus

variables. While discrimination accuracy of a one-octave difference in BW was 0.66 at best, that of a three-octave difference attained 0.95 (Fig. 2C, middle panel). Variations in the CF and BW are changes in lower-order image statistics (visible in the amplitude spectrum). The results therefore indicate that the tactile texture perception is sensitive to differences in low-order image statistics, although the tactile discrimination was not as good as the visual one (which is nearly perfect for the gray-level version of the stimuli).

For the third set, we printed textured surfaces transcribed from visual images of natural textures (i.e., irregular patterns of stones, leaves, actiniae, etc. Fig. 2A). We matched across textures the average and variance of the intensity (carving depth), while leaving the other statistical differences intact. Visually, five textures had very different spatial patterns. Nevertheless, the ten observers could barely discriminate most of the pairs by touch (Fig. 2C, bottom). Anecdotal reports from our observers suggest that the texture pattern (i.e., how the stimuli would look) was hard to guess and indistinguishable from other stimuli. The exception was NS3, which they described as somewhat 'spikier' than the rest. In summary, the same observers who could discriminate CF and BW stimuli could not discriminate most of the NS stimuli. Supplemental Fig. S1 shows the multi-dimensional scaling (MDS) of additional pairwise similarity judgments with CF, BW, and NS stimuli. In agreement with the results of the main discrimination experiment, NS stimuli are clustered in Fig. S1.

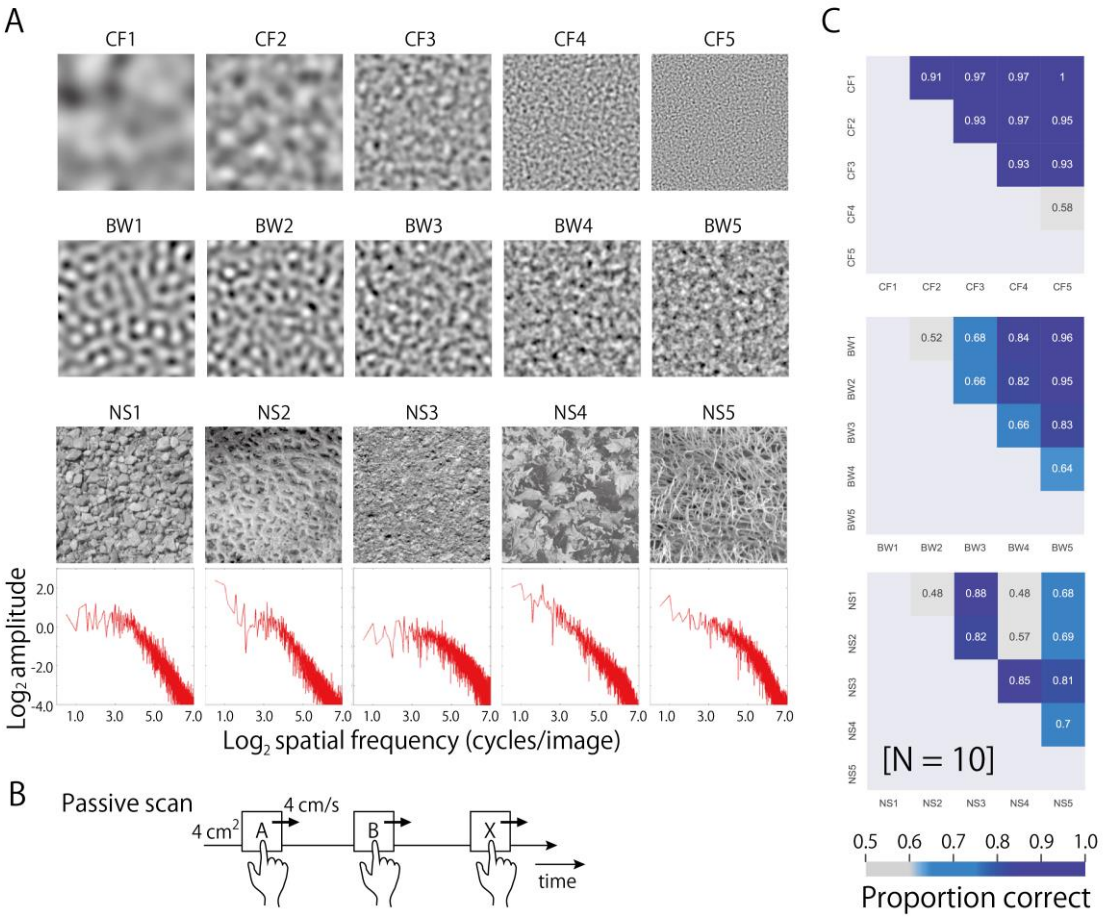

Fig. 2 ABX texture discrimination task for 3D-printed stimuli. (A) Visual images (256×256 pixels) were converted into 3D carvings (40×40×10-12 mm) by taking intensity values as height maps. The intensity level (the mean and standard deviation) was matched across images. The bottom panels are log amplitude spectra of NS images (i.e., the amplitude of each spatial frequency component in the Fourier spectrum, averaged across orientations. See also Fig. 4A for details.) (B) Time course of the ABX experiment. Passive scan condition. Observers placed their index finger on the first resting cushion and the linear stage started to move at 40 mm/sec. After the finger contacted the tactile stimulus and swiped for one second, the stage stopped on the next resting cushion. This was repeated three times, once each for an A, B and X stimulus, with X a rotated version of A or B. Observers were asked to report verbally whether the third stimulus was the first or second one. No feedback signal was provided. (C) Results. Discrimination performance (proportion correct) for each stimulus pair is shown by numbers and colors in a matrix format. The 95% confidence interval of the chance performance is 0.42-0.57 and that for 99.5% is 0.38-0.62

Since haptic performance is known to be significantly affected by the touching mode, we repeated our ABX experiment for NS stimuli with three other touching modes. In the main experiment,

we used the passive scan mode to match the speed and trajectory of scanning across different stimuli and different observers as much as possible. On the other hand, active scanning, in which observers can freely move their finger to explore the stimulus surface, may be able to provide richer spatial information than passive scanning (Kenshalo, 1978; Paillard et al., 1978). We therefore conducted the ABX experiment with the active scan mode. While the performance was slightly improved (average probability of 0.70 for passive scan; 0.76 for active scan, Fig. 3 left panel), the pattern of the results was similar to that in the passive scan condition. This is in good agreement with previous findings that tactile texture perception, including that of roughness and orientation, is relatively insensitive to changes in the exploration speed (Johnson and Yoshioka, 2002; Taylor and Lederman, 1975) and exploration method (Heller, 1989; Lamb, 1983; Olczak et al., 2018; Verrillo et al., 1999; Yoshioka et al., 2011). The other two modes were concerned with possible summation effects. Since the tactile system shows drastic spatial and temporal summation particularly with sub-threshold stimuli (Gescheider et al., 1999, 2005), texture discrimination performance might be seriously violated for complex textures like NS that give rapidly changing input in space and time. To reduce potentially negative effects of temporal/spatial summation on texture perception, we tested the static touch mode, where temporal information was limited, and the vibration mode, where spatial information was limited. In neither case did performance improve (Fig. 3, middle and right panels). In summary, the results indicate that some NS pairs are metameric regardless of the mode of touching. These trends across touching modes were the same for CF and BW stimuli (See Supplemental Fig. S2).

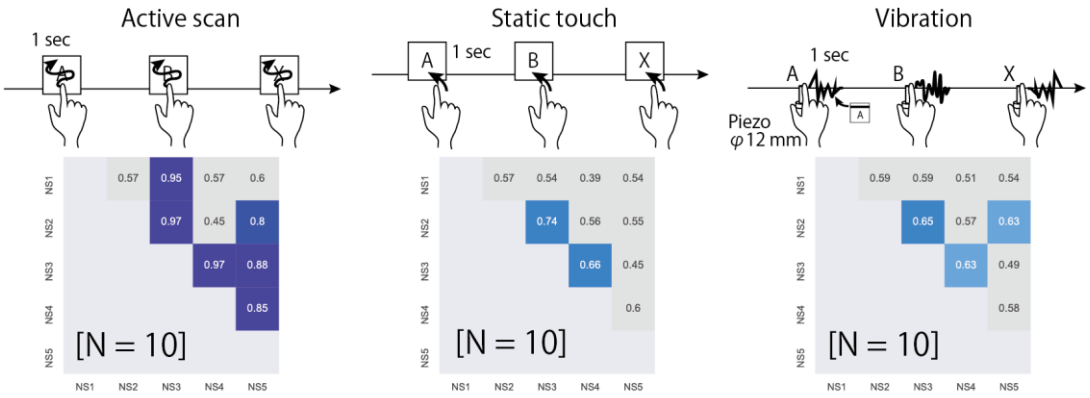

Fig. 3. Texture discrimination for NS stimuli with the other touching modes. In the active scan condition, observers could freely explore the stimuli for one second with their index finger. In the static touch condition, observers put their finger on the stimuli for one second. They were not allowed to tangentially move/scan their finger over the stimuli. In the vibration condition, observers' finger was vibrated by a piezo-electric actuator (MU120, MESS-TEK, Japan). The vibration pattern was one of the texture height profiles swept along a horizontal line. The observers could not discriminate some pairs of NS stimuli regardless of the touching mode.

The results obtained with the CF and BW stimuli indicate that tactile texture perception is sensitive to (some sorts of) differences in the amplitude spectrum or in the lower-order statistics. We next consider how well the discrimination performance for the NS stimuli can be explained by the differences in the amplitude spectrum. It is known that natural visual textures tend to have the amplitude spectrum falling with the spatial frequency by a factor of f^{-a} (Field, 1987). Our NS stimuli also have such amplitude spectra, which are similar to one another (Fig. 2A), although the slope of the spectrum differs for some textures. To analyze whether the similarity of amplitude spectra can explain the discrimination performance of tactile textures, we first integrated the amplitude differences between the paired textures over frequency (Fig. 4A) and then regressed the net amplitude difference to the discrimination performance by using a logistic regression analysis for all CF, BW, and NS conditions. Figure 4B shows the estimated performance plotted against the human performance. Although we did not consider orientation, the correlation was fairly high: R^2=0.65 and 0.81 for the overall correlation and NS condition correlation, respectively. That is, the more similar the amplitude spectrum was, the more difficult the tactile texture discrimination became.

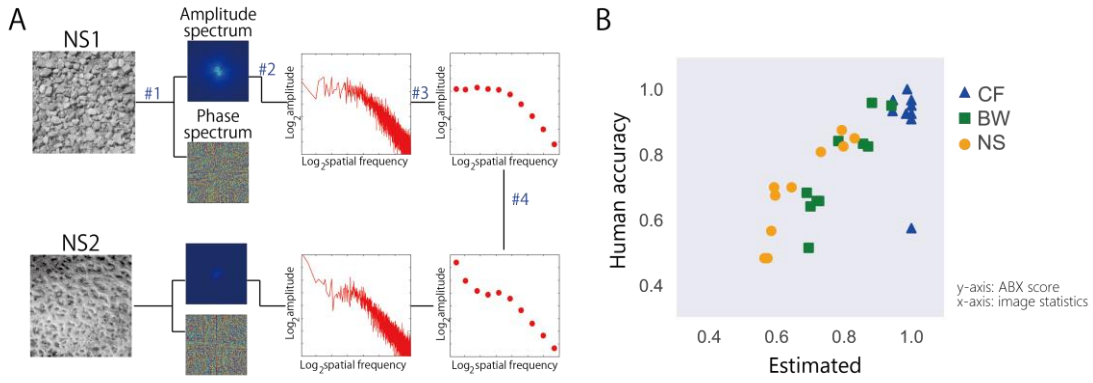

Fig. 4. The discrimination performance for the natural visual texture can be explained by the amplitude difference. (A) Calculation of the amplitude difference. Step1 [#1]: The amplitude spectrum of each texture image is calculated through a 2D fast Fourier transformation (FFT). Step 2 [#2]: The amplitude of each spatial frequency component is averaged across different orientations on a log scale. Step 3 [#3]: The amplitude spectrum is sampled at constant intervals. Step 4 [#4]: The differences between the amplitude spectra of paired textures are used to explain the discrimination performance in Fig. 2. (B) Correlation between the human discrimination performance in the passive scan condition and the performance estimated by logistic regression analysis based on amplitude differences.

The results obtained so far can be ascribed solely to tactile texture processing sensitive to lower-order statistics, suggesting a hypothesis that tactile texture processing is unable to use higher-

order statistics (e.g., joint Gabor statistics, phase spectra), to which visual texture perception is sensitive. This hypothesis predicts that textures with identical lower-order (subband) statistics are haptically indistinguishable (i.e., become a metameric pair) even if they differ from one another in the higher-order statistics. To test this, we made five images with identical subband histograms (Fig. 5A, bottom panels M1-M5) by matching the subband histogram of four NS images (NS2-NS5) to that of NS1 (based on Heeger and Bergen, 1995, see Methods). Visually, the matched images looked different from one another, and they were similar to the original images with regard to global patterning. However, haptic discrimination performance was nearly chance, 0.53 on average, and 0.61 at best. The result of the MDS analysis of the pairwise similarity ratings also supported this conclusion: NS stimuli are similar but somehow distributed in perceptual space, while they are concentrated around the base stimulus (NS1) when their histograms are matched (See Supplemental Fig. S3).

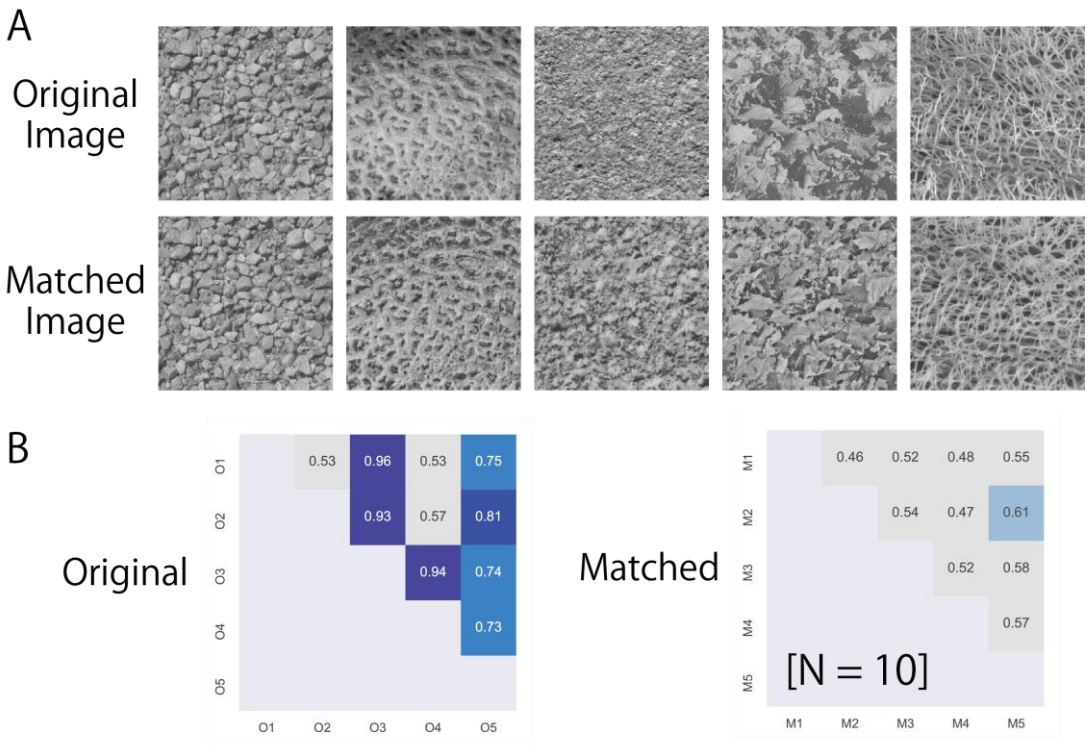

Fig. 5. Original and matched NS stimuli. (A) Original NS images and histogram-matched NS images. Matched stimuli (M1-5) were based on different original images (NS/O1-5) but shared the subband histogram of NS1. (B) Results. Observers who could discriminate a few pairs of original NS stimuli could not discriminate NS-matched stimuli.

General discussion

In this paper, our intent is to shed light on the similarities and differences in spatial-information processing mechanisms between vision and touch, the two major sensory modalities to perceive

surface textures. The main question is whether these mechanisms are qualitatively similar in processing or whether they differ according to the accessible levels of stimulus features/statistics. We directly examined whether human observers can detect differences in higher-order texture statistics of 3D-printed stimuli, whose height patterns were manipulated with regard to image statistics. The key finding was that observers were unable to discriminate surface textures as long as the textures shared the same lower-order statistics (e.g., subband histograms). Our tentative understanding here is that the tactile spatial pattern processor can take into account some statistics related to the local amplitude spectrum (level #1 and #2 in Fig. 1), including the center frequency and bandwidth, but not those related to the phase spectrum or joint statistics (at level #3 in Fig. 1). There are qualitative differences in spatial-information processing between vision and touch.

Simulation of skin deformation and neural activity in periphery

We wonder whether the observed insensitivity to the higher-order statistics reflects processing characteristics of the central nervous system or simple information loss in the periphery, i.e., the elasticity of the skin and noisy sparse sampling by mechanoreceptors. To make our best guess of how the difference in spatial texture information is represented in peripheral neural activation, we simulated responses of tactile afferents using the computational model 'TouchSim' (Saal et al., 2017). The beauty of this model is that it can provide the responses of hundreds of distributed afferents on a millisecond scale, though it works under some simplified assumptions (e.g., it does not incorporate lateral sliding/forces). Using this model, we examined whether sufficient information for texture discrimination remains at peripheral stages.

We simulated the spike timings and spatial distributions of the afferents while the index finger pad scanned our subband-matched NS stimuli. We calculated the firing similarity across stimuli in terms of a spike distance metric (Victor and Purpura, 1997), following the original 'TouchSim' study (Saal et al., 2017). We found that the firing similarities between pairs of identical texture stimuli with independent neural noise were always higher than those between pairs comprising two different stimuli, regardless of the type of afferent (Fig. 6). This suggests that an ideal central encoder of the peripheral signals, which could fully utilize information including higher-order statistics, would be able to discriminate subband-matched stimulus pairs. Therefore, our finding of insensitivity to the higher-order statistics likely reflects processing characteristics of the central nervous system rather than information loss in the periphery mechanisms. It should be noted that unlike in the psychophysical ABX task, we did not rotate the texture when comparing the simulated neural responses between identical stimuli. This is because the firing similarity measure we used does not explicitly compute the similarity in higher-order statistics represented in terms of the relationship between neighboring afferent firings.

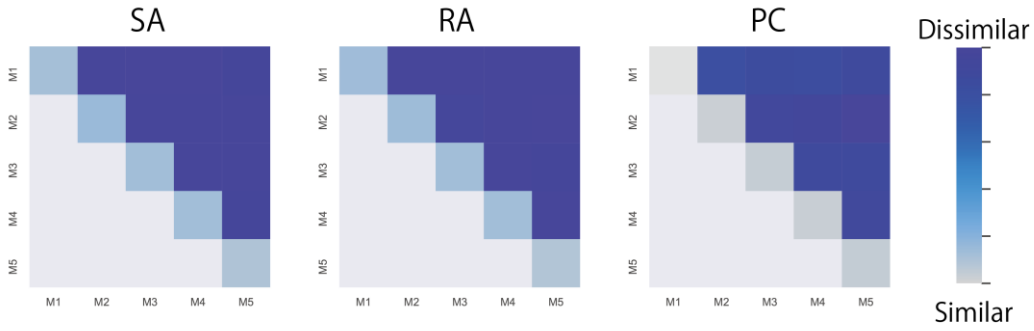

Fig. 6. Similarity of neural firing patterns when the subband-matched stimuli were touched. The responses of tactile fibers of the index finger pad to NS-matched stimuli were simulated by the computational model 'TouchSim' (Saal et al., 2017). The similarity of simulated neural firing patterns was evaluated in terms of the Victor distance (Victor and Purpura, 1997). The distance between simulated firings was smaller (lighter colour) when the same stimulus (diagonal patches) was scanned than when two different stimuli were scanned (darker colour). See detail in method.

Relationship with roughness perception

Roughness has been explored extensively and is recognized as a major feature in haptic texture perception (Bensmaia, 2009; Klatzky et al., 2013; Hollins et al., 1993, 2000; Tiest, 2010; Tiest and Kappers, 2006). Past studies have reported a variety of properties of roughness perception, including remarkable discrimination performance—we can detect even nanometre-scale differences (Skedung et al., 2013). Concerning the relationship with the current study, roughness perception can be ascribed to the tactile responses to lower-feature statistics, such as density or the deviation of surface elements (#1, #2 in Fig.1). As far as we are aware, the known characteristics of texture roughness perception do not conflict with our hypothesis that the tactile system is insensitive to higher-order feature statistics. Compared with the texture patterns used in previous roughness studies, the ones used in the current study were much more complex. In addition, our observers could use texture differences in dimensions other than roughness to accomplish the ABX discrimination task. However, we do not exclude a possibility that they mainly relied on what previous studies called roughness in performing the discrimination task. We therefore considered whether the current results can be accounted for by previously proposed roughness indexes. Since the carving depth (the mean and standard deviation) was normalized and equated across our NS stimuli, industrial indexes of surface roughness, such as the arithmetical mean height of a surface (Ra) and maximum height of a surface (Rz), cannot explain the discrimination performance for the NS stimuli (Kuroki et al., 2018). Other types or roughness indexes are based on neural responses. We computed two neural roughness indexes—the mean impulse rate of high-frequency PC afferents (Bensmaia & Hollins, 2005; Hollins & Bensmaia, 2007) and spatial variation of low-frequency SA afferents (Connor et al., 1990, 1992)—from the output of

'TouchSim'. Note that these indexes do not take into account higher-order statistics, so we did rotate the texture and add spatial jitter derived from contact position variability when repeating the simulated neural responses. We found the simulated indexes to indicate similar or even higher discrimination performance for NS-original and NS-matched stimuli compared to the observed behavioural performance (See Supplemental Fig. S4). The predictions of these indexes might be improved by adjustment of noise parameters. Further investigation is warranted to determine how well these or other neural roughness indexes can explain tactile perception of complex texture patterns like the ones we introduced.

Relationship with shape perception

Although our findings indicate that tactile *texture* perception is insensitive to higher-order statistics, they do not exclude a possibility that tactile *shape* perception has sensitivity to some higher-order features. Tactile shape perception shows high sensitivity to stimulus orientation. Edge orientation acuity was reported to be around 20 degrees (Bensmaia et al., 2008; Olczak et al., 2018) or even smaller (Pruszynski et al., 2018). Furthermore, human touch can discriminate more complex spatial patterns such as letters of the alphabet. The performance of tactile letter recognition is reported to be fairly high and positively correlated with its visual counterpart (Craig, 1979). One may interpret this result to suggest the ability of the tactile shape perception to discriminate some spatial phase differences. Tactile shape perception and tactile texture perception have been studied nearly independently by using different types of stimuli. Shape perception has been tested with simple/local stimuli such as raised simple line/curvature patterns, while texture perception has been tested with complex/global stimuli, including natural textures. While shape perception focuses on a specific location in the stimulus, texture perception should grasp the holistic statistical nature of the field under crowding conditions as in the current experiments. We therefore do not assume that texture perception can be explained by the same mechanism as that for shape perception. Indeed, shape processing and texture processing may be segregated in somatosensory cortex. Cutaneous inputs are initially processed in primary somatosensory cortex — starting from Brodmann areas 3b to 1 and 2 — and are known to be hierarchically processed (See review for Delhaye et al., 2018; Sathian, 2016). Neurons in areas 3b and 1 show both roughness and orientation tuning, while those in higher areas such as area 2 (Fitzgerald et al., 2006; Yau et al., 2013) and parietal opercular cortex (Yau et al., 2009) show sensitivity to higher-order shape features (i.e., particular curvatures). Lesions in parietal opercular cortex are known to impair shape recognition but not roughness recognition (Roland, 1987), suggesting independence of these two processes. At present, we have no evidence of the contribution of a neural mechanism sensitive to higher-order features (curvature) to surface texture perception.

Future directions

To analyze the sensitivity of the tactile system to image statistics using a method similar to that used in vision research, we transcribed gray-scale visual images into surface depth maps. Due to the difference in the sensing process, however, we can only assume a rough correspondence of the sensor response pattern between the two modalities. To overcome this limitation, we used 'TouchSim' (Saal et al., 2017) to evaluate our hypothesis in this study, but more direct evaluation would be necessary in future.

Overall reversal of the signal sign (contrast polarity) affects some low-level statistics (e.g., the intensity histogram), but not the local amplitude spectrum. It is known that visual texture perception is sensitive to the sign of the input signals — it responds to positive (white) and negative (black) elements in an asymmetric way (e.g., Chubb et al., 2007). The signal sign may have even have stronger effects on our tactile stimuli, since a sign reversal swaps convex elements with concave ones, thereby introducing a large change in skin deformation patterns in particular for texture patterns consisting mainly of pin or hole elements. Indeed, we found that human observers could discriminate the original and the sign-reversal version for our NS stimuli (See Supplemental Fig. S5). This finding is obviously inconsistent with the idea that tactile texture discriminability is predicted by the local amplitude spectrum of the stimulus depth map. However, it may not be inconsistent with our basic hypothesis that low-level image statistics as represented by population activation in the primary somatosensory cortex is sufficient to predict tactile texture discriminability. The problem here is that precipitous height patterns are not precisely transferred to sensor response patterns due to the intermediate finger skin mechanism. One way to cope with this problem is to insert a non-linear mapping process between stimulus depth maps and sensor responses. For example, half-wave rectification of a texture pattern (leaving convex signals only) before calculating the amplitude spectrum will produce a significant difference between the original and sign-reversed version.

To have good control over higher-order image statistics of texture patterns, we used natural visual images carved on plastic-like material, and found them hard to discriminate by touch. One might suspect that the reason we failed to find tactile sensitivity to higher-order statistics was because we used textures very unnatural to the tactile system. Isn't the tactile system sensitive to higher-order image statistics that are useful in discriminating and recognizing natural textures we touch in our daily lives? Are higher-order image statistics potentially available for the human tactile system informative at all for daily tactile perception? To address these questions, it is necessary to sample and analyze image properties of numerous natural haptic textures we daily encounter.

A small number of our observers could distinguish some pairs of NS-matched stimuli (See supplemental Fig. S6). Whether they could successfully detect certain higher-order statistics or they just used conspicuous local features to solve the task remains unknown, and warrants further investigation.

The current findings may have implications for haptic engineering, where information reduction is essential. Some studies in this area tried to record and reproduce texture sensations. Wiertlewski et al. (2011) physically recorded vibrations between the finger and some flat or regularly grated stimuli and reproduced them without considering the phase/distribution. They found good correlation in discrimination ability between the original stimuli and their reproductions. They concluded that what is important in texture perception is spatial spectrograms, i.e., amplitude and spectral information. This is in good agreement with our results.

From a general viewpoint, the current finding may be compatible with the recent findings that the human tactile system is able to average textural information over different skin locations (Kahrimanovic et al., 2009; Kuroki et al., 2017; Rahman and Yau, 2019), in that all of these findings indicate that tactile texture perception is based on relatively simple averaging computation. This hypothesis warrants further investigation.

Concluding remarks

Recent 3D printing technology allows us to control the spatial pattern of tactile stimuli as accurately and flexibly as in the case of visual stimuli. This powerful methodology makes it possible to apply a variety of experimental paradigms developed in vision research to tactile research. As we demonstrated here, 3D printers will be powerful tools for future investigations of tactile spatial computation.

Several studies have investigated the relationship of touch with vision, as this study did. While several past influential studies (Amedi et al., 2001; Kitada et al., 2006; Merabet, 2004; Yau et al., 2009; Zangaladz et al., 1999) emphasized the similarities between the two modalities, our study rather highlighted the differences (see also Lederman et al., 1990; Whitaker et al., 2008). By doing so, we could clarify in what way spatial sensation by touch is different from spatial sensation by vision. While many people may share the intuition that tactile texture sensation is qualitatively different from visual texture sensation, here we showed, for the first time, that the qualitative differences arise from (in)sensitivity to higher-order image statistics.

Methods

Generating visual texture stimuli

Since our tactile stimuli were created by 3D-printing according to a height map, we dealt with the height map as a visual image and controlled its image statistics as in the visual texture literature. The image we used was either artificial Gaussian band-pass noise or a natural scene texture. For the artificial noise, we first applied the two-dimensional fast Fourier transform to a white noise image and extracted specific spatial frequency components by using a two-dimensional Gaussian band-path filter. There were two stimulus conditions of filter parameter manipulation: the center frequency (CF) and

bandwidth (BW) conditions (Fig. 2A, top and center). The CF condition used five center frequencies of the band-path filter (2, 4, 8, 16, and 32 cycles/image) while keeping the BW 1.5 octaves. The BW condition used five filter bandwidths (0.5, 1.0, 1.5, 2.0, and 2.5) while keeping the CF 8 cycles/image. In addition to the artificial noise, we used the natural scenes (NSs). For this NS condition, five images were chosen from the natural texture category of the McGill Calibrated Colour Image Database (Olmos and Kingdom, 2004). The intensity level (the mean and standard deviation) were normalized and equalized across images (Fig. 2A, bottom).

Generating tactile texture stimuli

Tactile stimuli were custom-built for the experiment by using a 3D printer (16-micrometer resolution) (Objet 260 Connex3, Stratasys, USA) with transparent plastic-like material (VeroClear-RGD810, Objet, USA). Each visual texture stimulus was converted into a 3D model by taking intensity values as a height map. The printed object was 40×40×10-12 mm. The contrast difference between complete black (0) and complete white (255) in an image was transcribed to a height (thickness of stimuli; black means deep) difference of 2 mm. Printing accuracy, measured with a wide-area 3D measurement system (VR-3100, KEYENCE, Japan), was within 0.056 mm on average. Prior to the experiment, the surface of the stimuli was lightly covered with baby powder (Baby Powder, Johnson & Johnson, USA) to ensure constant contact between the finger and stimuli by avoiding large stick-slips.

Generating tactile vibration stimuli

A piezoelectric actuator (MU120, MESS-TEK, Japan) was used as stimulator to reproduce the line scan of the texture height profile swept along a horizontal line. The stimulator normally deformed the skin with a maximum of 800 N force vibrated by a position control method so that it could accurately produce the required displacement with a tolerance of few nanometers. The diameter of the stimulator was 12.0 mm, and its edges were separated from the rigid surround of the metal boards by a 1.0-mm gap (following (Verrillo, 1963)). The rigid surround limits the spread of surface waves of the skin. The stimulator always contacted the finger throughout the experiment. The line on the textured surface to be converted into vibration was randomly chosen for each trial. Note that due to actuator limitations, the original height difference was linearly reduced to fit within 120 μm (roughly 1/10 scale).

Subjects

Thirty-eight naïve observers and two of the authors (12 males) with normal tactile sensitivity (by self-reports), aged from 21 to 46 years (32.3±7.66) participated the experiments. All gave informed consent approved by the NTT Communication Science Laboratory Research Ethics Committee, and all procedures were conducted in accordance with the Declaration of Helsinki.

Procedures

ABX experiment with CF, BW, and NS modulation.

Groups of ten observers participated for each passive, active, static, and vibration condition, with partial overlaps of observers across conditions. An observer sat at a table and placed the index finger of the right hand on home position with their right arm on an arm rest. They performed experiments with eyes open to maintain their arousal level, but they could not see the tactile stimuli, the equipment, nor experimenter, which were occluded by a black curtain.

In general, observers touched three stimuli, A, B, and X, each for one second, where X was a rotated version of A or B, and they verbally reported which one was X, the first or second. Since X was rotated, observers could not perform feature matching using trivial keys. Paired stimuli (A and B) were randomly chosen from five stimuli of the same modulation (CF, BW, or NS). This procedure is called an ABX task (Kingdom & Prins, 2010), and one of the advantages of this task is that it is less affected by labeling problems. If the observers are asked to directly evaluate the similarity between paired stimuli, these stimuli must be labeled, and their responses may be influenced by labeling difficulties and/or confusion between labels. On the other hand, with the ABX task, the observer can report the relative similarity between X and A and X and B, even if A and B are not clearly labeled.

There were four different touching mode conditions. Other than in the vibration condition, the experimenter set three predetermined stimuli (A, B, X) on a linear stage (ERL2, CKD, Japan) before each trial started. By automatically moving the stage, the experimenter was able to guide the three stimuli directly beneath the finger. Thus, observers did not have to move the wrist to touch them. In the passive scan condition, each trial started with the experimenter's 'ready' call. An observer put their right index finger at the rest position at the right edge of the linear stage and pressed the start button on the PC monitor with their left hand to trigger the stage movement. The linear stage started to move under observers' right index finger from left to right for approximately 1.5 seconds with a speed of 40 mm/s so that the rightmost one of three stimuli swiped the finger for one second. After a one second pause, the stage automatically moved again for the second stimulus to swipe, stopped, then moved again for the third stimulus to swipe. After the third scan, observers lifted their fingers and made a binary verbal report as to which of the first two stimuli (the first or the second) was the same to the last one. The stage moved back to its initial position and the experimenter changed the stimuli on the stage for the next trial. In active scan condition, observers lifted their right index finger above the first stimulus position and pressed the start button. They freely scanned the stimulus surface for one second and lifted their finger again. Then, the stage started to move and the second stimuli came right under their finger. Observers never touched the stimuli when the stage was moving; they touched them three times each for one second when the stage had stopped. In the static touch condition, observers put their fingers on static (not moving) stimuli three times each for one second, in similar time course to other conditions. In the vibration condition, the stage and stimuli were replaced with the piezoelectric

actuator. Observers placed their right index finger on the actuator and pressed the start button on the monitor with their left hand. After about one second, the actuator vibrated three times each for one second with 1.5-second gap. Only in this condition did observers report by button clicking instead of verbally. To mask any subtle sound made by the actuator, observers wore ear plugs and white noise was played continuously from headphones throughout this condition.

There were three kinds of modulation (CF, BW, and NS), five modulation gradations, four touching modes (passive scan, active scan, static touch, and vibration), and 12 repetitions for each combination. In total, 360 trials were conducted for each touching mode, and sessions were roughly divided into ten blocks. No block lasted longer than 15 minutes. Within each block, the kind of modulation and the gradations were randomized and the touching mode was fixed.

ABX experiment with NS original and NS matched modulation.

Ten observers participated. The equipment and procedure were almost identical to those of the passive scan condition in the ABX experiment, except for the stimulus. The experiment was conducted with two kinds of modulation (original and matched NS), five modulation gradations, one touching mode (passive scan), and 12 repetitions for each combination.

Logistic regression analysis based on amplitude differences.

To investigate whether the discrimination performance can be explained by the amplitude differences in the textures, we used a logistic regression analysis. As shown in Fig. 4A, the amplitude of each spatial component was calculated on a log scale and sampled to ten points in 0.7-octave intervals. The difference between the amplitude spectra of paired textures was calculated at each sampled point. We used the ten values as predictor variables for each discrimination performance as follows.

$$\hat{\beta} = \underset{\beta}{argmin}\left[\sum_{i}^{N}\left(\frac{1}{1+exp\left(-\sum_{k}^{P}\beta(k)x(i,k)\right)} - y(i)\right)^2\right], \quad \beta(k) \geq 0$$

,

where x is the predictor variable, β its coefficients, y the human discrimination accuracy for each pair, N the number of pairs, and P the number of the predictor variables. We used Matlab function *fmincon* for the optimization. By the sparse logistic regression, five of the ten predictor variables survived, and were used in estimating the performance shown in Fig. 4B.

Generating the subband-matched images

To test if textures with identical lower-order (subband) statistics were haptically indistinguishable, we made five images with identical subband histograms (Fig. 5A, bottom panels M1-M5) by using a texture synthesis algorithm (Heeger & Bergen, 1995). In this algorithm, the steerable pyramid transform is utilized. Specifically, each image was decomposed into several spatial-frequency and orientation bands by convolving the image with spatially oriented linear filters and by subsampling. Using the transformed subbands, this algorithm synthesizes the texture by matching the histograms of transform coefficients of the seed image to those of the target image. We used original image 1 (NS/O1) as the target for the synthesis. The original algorithm uses a white noise image as the seed image. However, since we aimed to make a set of textures while preserving the higher order statistics of each original texture (O1 - O5), we used the original texture as the seed image. To make the matched images in Fig. 5, we adopted four spatial frequencies bands and four orientation bands.

Simulation

We simulated spatio-temporally distributed firing patterns of three different types of tactile afferent by using the computational model "TouchSim", which can reproduce major response characteristics that have been clarified by previous research (Saal et al., 2017). The original parameters of the model were based on measured spiking data obtained with monkeys. The simulated responses of afferents closely match the known spiking responses of actual afferents (both precise millisecond spike-timings and firing rates) to various classes of stimuli (for example, vibrations, edges, and textured surfaces).

Responses to NS matched stimuli were simulated. The stimulus was scanned across the skin. The contact area was defined as a rectangle (20-mm length and 10-mm width) and the resolution (input spacing, defined as pin spacing in 'TouchSim') was set to 0.1 mm. The skin contact area was indented at the center of the index fingertip with the averaged depth of 1 mm, moved across the stimuli at a speed of 40 mm/s for one second. Realistically distributed afferents (288 SA, 569 RA, and 102 PC in index fingertip 'D2d') were simulated with a 1-ms resolution. The simulation was repeated 12 times for each stimulus, with afferent distribution, stimulus contact area, and scan direction fixed.

Since we simulated temporally and spatially distributed firings, higher-order statistical information, if any, should be embedded in the firing pattern. To quantitatively test whether this pattern is similar when touching the same stimulus compared to when touching different stimuli, we conducted metric space analysis. In particular, we calculated the Victor distance (Victor and Purpura, 1997) following the previous 'TouchSim' study (Saal et al., 2017). This analysis enables us to compare the similarity of the timing of the spikes by introducing cost parameter q, which we set to 100 (corresponding to 10 ms) in this study. For each afferent model, the Victor distance was calculated between all pairwise combinations of the simulated trials for five stimuli. Obtained distances were normalized by the total number of spikes in the pair and then averaged for the same kind of afferent model and for the same pair of stimuli (Fig. 6).

Acknowledgment

This work was supported by Grant-in-Aid for Scientific Research on Scientific Research on Innovative Areas "Shitsukan" (No. 15H05915) from MEXT, Japan.

Reference

1. Julesz, B. (1962). Visual Pattern Discrimination. *IEEE Transactions on Information Theory*, *8*(2), 84–92.
2. Bergen, J. R., & Adelson, E. H. (1988). Early vision and texture perception. *Nature*, *333*(6171), 363–364. http://doi.org/10.1038/333363a0
3. Freeman, J., & Simoncelli, E. P. (2011). Metamers of the ventral stream. *Nature Neuroscience*, 14(9), 1195–1201. http://doi.org/10.1038/nn.2889
4. Freeman, J., Ziemba, C. M., Heeger, D. J., Simoncelli, E. P., & Movshon, J. A. (2013). A functional and perceptual signature of the second visual area in primates. *Nature Neuroscience*, *16*(7), 974–981. http://doi.org/10.1038/nn.3402
5. Ziemba, C. M., Freeman, J., Movshon, J. A., & Simoncelli, E. P. (2016). Selectivity and tolerance for visual texture in macaque V2. *Proc Natl Acad Sci USA*, *113*(22), E3140–E3149.
6. Rosenholtz, R. (2016). Capabilities and Limitations of Peripheral Vision. *Annual Review of Vision Science*, *2*(1), 437–457. http://doi.org/10.1146/annurev-vision-082114-035733
7. Klein, S. A., & Tyler, C. W. (1986). Phase discrimination of compound gratings: Generalized autocorrelation analysis. Journal of the Optical Society of America A, Optics and Image Science, 3, 868–879.
8. Hansen, B. C., & Hess, R. F. (2006). Discrimination of amplitude spectrum slope in the fovea and parafovea and the local amplitude distributions of natural scene imagery. *Journal of Vision*, 6(7), 696-711.
9. Delhaye, B. P., Long, K. H., & Bensmaia, S. J. (2018). Neural Basis of Touch and Proprioception in Primate Cortex. *Comprehensive Physiology*, *8*(4), 1575.
10. Pruszynski, J. A., & Johansson, R. S. (2014). Edge-orientation processing in first-order tactile neurons. *Nature Neuroscience*, *17*(10), 1404–1409. https://doi.org/10.1038/nn.3804
11. Bensmaia, S. J., Denchev, P. V, Dammann, J. F., Craig, J. C., & Hsiao, S. S. (2008). The representation of stimulus orientation in the early stages of somatosensory processing. *Journal of Neuroscience*, *28*(3), 776–786.

12. DiCarlo, J. J., Johnson, K. O., & Hsiao, S. S. (1998). Structure of receptive fields in area 3b of primary somatosensory cortex in the alert monkey. *J Neurosci*, *18*(7), 2626–2645.
13. DiCarlo, J. J., & Johnson, K. O. (2000). Spatial and temporal structure of receptive fields in primate somatosensory area 3b: effects of stimulus scanning direction and orientation. *J Neurosci*, *20*(1), 495–510. Retrieved from http://www.ncbi.nlm.nih.gov/entrez/query.fcgi?cmd=Retrieve&db=pubmed&dopt=Abstract&list_uids=10627625
14. Thakur, P. H., Fitzgerald, P. J., Lane, J. W., & Hsiao, S. S. (2006). Receptive field properties of the macaque second somatosensory cortex: nonlinear mechanisms underlying the representation of orientation within a finger pad. *Journal of Neuroscience*, *26*(52), 13567–13575.
15. Yau, J. M., Pasupathy, A., Fitzgerald, P. J., Hsiao, S. S., & Connor, C. E. (2009). Analogous intermediate shape coding in vision and touch. *Proceedings of the National Academy of Sciences*, *106*(38), 16457–16462.
16. Bensmaia, S. (2009). Texture from touch. *Scholarpedia*, *4*(8), 7956.
17. Klatzky, R. L., Pawluk, D., & Peer, A. (2013). Haptic perception of material properties and implications for applications. *Proceedings of the IEEE*, *101*(9), 2081–2092.
18. Holliins, M., Faldowski, R., Rao, S., & Young, F. (1993). Perceptual dimensions of tactile surface texture: A multidimensional scaling analysis. *Perception & Psychophysics*, *54*(6), 697–705.
19. Hollins, M., Bensmaia, S., Karlof, K., & Young, F. (2000). Individual differences in perceptual space for tactile textures: Evidence from multidimensional scaling. *Perception & Psychophysics*, *62*(8), 1534–1544.
20. Tiest, W. M. B. (2010). Tactual perception of material properties. *Vision Research*, *50*(24), 2775–2782.
21. Tiest, W. M. B., & Kappers, A. M. L. (2006). Analysis of haptic perception of materials by multidimensional scaling and physical measurements of roughness and compressibility. *Acta Psychologica*, *121*(1), 1–20.
22. Goodwin, A. W., John, K. T., Sathian, K., & Darian-Smith, I. (1989). Spatial and temporal factors determining afferent fiber responses to a grating moving sinusoidally over the monkey's fingerpad. *Journal of Neuroscience*, *9*(4), 1280–1293.
23. Lederman, S. J. (1983). Tactual roughness perception: Spatial and temporal determinants. *Canadian Journal of Psychology/Revue Canadienne de Psychologie*. https://doi.org/10.1037/h0080750

24. Lederman, S. J., & Taylor, M. M. (1972). Fingertip force, surface geometry, and the perception of roughness by active touch. *Perception & Psychophysics*, *12*(5), 401–408.
25. Sathian, K., Goodwin, A. W., John, K. T., & Darian-Smith, I. (1989). Perceived roughness of a grating: correlation with responses of mechanoreceptive afferents innervating the monkey's fingerpad. *Journal of Neuroscience*, *9*(4), 1273–1279.
26. Taylor, M. M., & Lederman, S. J. (1975). Tactile roughness of grooved surfaces: A model and the effect of friction. *Perception & Psychophysics*, *17*(1), 23–36. https://doi.org/10.3758/BF03203993
27. Yau, J. M., Connor, C. E., & Hsiao, S. S. (2013). Representation of tactile curvature in macaque somatosensory area 2. *American Journal of Physiology-Heart and Circulatory Physiology*.
28. Bensmaia, S., & Hollins, M. (2005). Pacinian representations of fine surface texture. *Perception & Psychophysics*, *67*(5), 842–854
29. Hollins, M., & Bensmaia, S. J. (2007). The coding of roughness. *Canadian Journal of Experimental Psychology/Revue Canadienne de Psychologie Experimentale*, *61*(3), 184.
30. Weber, A. I., Saal, H. P., Lieber, J. D., Cheng, J.-W., Manfredi, L. R., Dammann, J. F., & Bensmaia, S. J. (2013). Spatial and temporal codes mediate the tactile perception of natural textures. *Proceedings of the National Academy of Sciences*, *110*(42), 17107–17112. https://doi.org/10.1073/pnas.1305509110
31. Yokosaka, T., Kuroki, S., Watanabe, J., & Nishida, S. (2017). Linkage between free exploratory movements and subjective tactile ratings. *IEEE Transactions on Haptics*, *10*(2), 217–225.
32. Kingdom, F. A .A. & Prins, N. (2010) *Psychophysics: A Practical Introduction*. Academic Press: an imprint of Elsevier, London.
33. Freeman, J., & Simoncelli, E. P. (2011). Metamers of the ventral stream. *Nature Neuroscience*, *14*(9), 1195–1204. https://doi.org/10.1038/nn.2889
34. Bolanowski Jr, S. J., Gescheider, G. A., Verrillo, R. T., & Checkosky, C. M. (1988). Four channels mediate the mechanical aspects of touch. *The Journal of the Acoustical Society of America*, *84*(5), 1680–1694.
35. Gescheider, G. A., Bolanowski, S. J., & Hardick, K. R. (2001). The frequency selectivity of information-processing channels in the tactile sensory system. *Somatosensory and Motor Research*, *18*(3), 191–201. https://doi.org/10.1080/01421590120072187
36. Gescheider, G. A., Bolanowski, S. J., Pope, J. V., & Verrillo, R. T. (2002). A four-channel analysis of the tactile sensitivity of the fingertip: Frequency selectivity, spatial

summation, and temporal summation. *Somatosensory and Motor Research*, *19*(2), 114–124. https://doi.org/10.1080/08990220220131505

37. Kenshalo, D. R. (1978). Biophysics and psychophysics of feeling. In E.C. Carterette & M.P. Friedman (Eds.) *Handbook of perception, Feeling and Hurting*. New York: Academic Press. https://doi.org/10.1016/C2013-0-10470-9
38. Paillard, J., Brouchon-Viton, M., & Jordan, P. (1978). Differential encoding of location cues by active and passive touch. *Active Touch*, 189–196.
39. Johnson, K. O., & Yoshioka, T. (2002). *Neural mechanisms of tactile form and texture perception*. na.
40. Heller, M. A. (1989). Texture perception in sighted and blind observers. *Perception & Psychophysics*, *45*(1), 49–54.
41. Lamb, G. D. (1983). Tactile discrimination of textured surfaces: psychophysical performance measurements in humans. *The Journal of Physiology*, *338*(1), 551–565..
42. Olczak, D., Sukumar, V., & Pruszynski, J. A. (2018). Edge orientation perception during active touch. *Journal of Neurophysiology*, *120*(5), 2423–2429.
43. Verrillo, R. T., Bolanowski, S. J., & McGlone, F. P. (1999). Subjective magnitude of tactile roughness. *Somatosensory & Motor Research*, *16*(4), 352–360.
44. Yoshioka, T., Craig, J. C., Beck, G. C., & Hsiao, S. S. (2011). Perceptual Constancy of Texture Roughness in the Tactile System. *Journal of Neuroscience*, *31*(48), 17603–17611. https://doi.org/10.1523/JNEUROSCI.3907-11.2011
45. Gescheider, G.A., Berryhill, M. E., Verrillo, R. T., & Bolanowski, S. J. (1999). Vibrotactile temporal summation: probability summation or neural integration? *Somatosensory & Motor Research*, *16*(3), 229–242.
46. Gescheider, G. A., Güçlü, B., Sexton, J. L., Karalunas, S., & Fontana, A. (2005). Spatial summation in the tactile sensory system: Probability summation and neural integration. *Somatosensory and Motor Research*, *22*(4), 255–268. https://doi.org/10.1080/08990220500420236
47. Field, D. J. (1987). Relations between the statistics of natural images and the response properties of cortical cells. *Journal of the Optical Society of America. A, Optics and Image Science*, *4*(12), 2379–2394. https://doi.org/10.1364/JOSAA.4.002379
48. Heeger, D. J., & Bergen, J. R. (1995, September). Pyramid-based texture analysis/synthesis. In *Proceedings of the 22nd annual conference on Computer graphics and interactive techniques* (pp. 229-238). ACM.
49. Saal, H. P., Delhaye, B. P., Rayhaun, B. C., & Bensmaia, S. J. (2017). Simulating tactile signals from the whole hand with millisecond precision. *Proceedings of the National Academy of Sciences*, *114*(28), E5693--E5702.

50. Victor, J. D., & Purpura, K. P. (1997). Metric-space analysis of spike trains: theory, algorithms and application. *Network: Computation in Neural Systems*, *8*(2), 127–164.
51. Holliins, M., Faldowski, R., Rao, S., & Young, F. (1993). Perceptual dimensions of tactile surface texture: A multidimensional scaling analysis. *Perception & Psychophysics*, *54*(6), 697–705.
52. Skedung, L., Arvidsson, M., Chung, J. Y., Stafford, C. M., Berglund, B., & Rutland, M. W. (2013). Feeling small: exploring the tactile perception limits. *Scientific Reports*, *3*, 2617.
53. Kuroki, S., Sawayama, M., & Nishida, S. (2018). Haptic Texture Perception on 3D-Printed Surfaces Transcribed from Visual Natural Textures. In *International Conference on Human Haptic Sensing and Touch Enabled Computer Applications* (pp. 102–112).
54. Connor, C. E., Hsiao, S. S., Phillips, J. R., & Johnson, K. O. (1990). Tactile roughness: neural codes that account for psychophysical magnitude estimates. *The Journal of Neuroscience : The Official Journal of the Society for Neuroscience*, *10*(12), 3823–3836. https://doi.org/http://www.ncbi.nlm.nih.gov/pubmed/2269886
55. Connor, C. E., & Johnson, K. O. (1992). Neural coding of tactile texture: comparison of spatial and temporal mechanisms for roughness perception. *Journal of Neuroscience*, *12*(9), 3414–3426.
56. Pruszynski, J. A., Flanagan, J. R., & Johansson, R. S. (2018). Fast and accurate edge orientation processing during object manipulation. *Elife*, *7*, e31200.
57. Craig, J. C. (1979). A confusion matrix for tactually presented letters. *Attention, Perception, & Psychophysics*, *26*(5), 409–411.
58. Sathian, K. (2016). Analysis of haptic information in the cerebral cortex. *Journal of Neurophysiology*, *116*(4), 1795–1806.
59. Fitzgerald, P. J., Lane, J. W., Thakur, P. H., & Hsiao, S. S. (2006). Receptive field (RF) properties of the macaque second somatosensory cortex: RF size, shape, and somatotopic organization. *Journal of Neuroscience*, *26*(24), 6485–6495.
60. Roland, P. E. (1987). Somatosensory detection of microgeometry, macrogeometry and kinesthesia after localized lesions of the cerebral hemispheres in man. *Brain Research Reviews*, *12*(1), 43–94.
61. Chubb, C., Nam, J.-H., Bindman, D. R., & Sperling, G. (2007). The three dimensions of human visual sensitivity to first-order contrast statistics. Vision Research, 47(17), 2237–2248. http://doi.org/10.1016/j.visres.2007.03.025

62. Wiertlewski, M., Lozada, J., & Hayward, V. (2011). The spatial spectrum of tangential skin displacement can encode tactual texture. *IEEE Transactions on Robotics*, *27*(3), 461–472.
63. Kahrimanovic, M., Bergmann Tiest, W. M., & Kappers, A. M. L. (2009). Context effects in haptic perception of roughness. *Experimental Brain Research*, *194*(2), 287–297. https://doi.org/10.1007/s00221-008-1697-x
64. Kuroki, S., Watanabe, J., & Nishida, S. (2017). Integration of vibrotactile frequency information beyond the mechanoreceptor channel and somatotopy. *Scientific Reports*, *7*(1), 2758. https://doi.org/10.1038/s41598-017-02922-7
65. Rahman, M. S., & Yau, J. M. (2019). Somatosensory interactions reveal feature-dependent computations. *Journal of Neurophysiology*. https://doi.org/10.1152/jn.00168.2019
66. Amedi A, Malach R, Hendler T, Peled S, Zohary E (2001) Visuo-haptic object-related activation in the ventral visual pathway. *Nat Neurosci* 4:324–330.
67. Kitada R, et al. (2006) Multisensory activation of the intraparietal area when classifying grating orientation: A functional magnetic resonance imaging study. *J Neurosci* 26:7491–7501.
68. Merabet L, et al. (2004) Feeling by sight or seeing by touch? *Neuron* 42:173–179.
69. Zangaladze A, Epstein CM, Grafton ST, Sathian K (1999) Involvement of visual cortex in tactile discrimination of orientation. *Nature* 401:587–590.
70. Lederman S. J., Klatzky R. L., Chataway C, Summers C. D. (1990) Visual mediation and the haptic recognition of two-dimensional pictures of common objects. *Percept Psychophys* 47(1), 54-64.
71. Whitaker T. A., Simões-Franklin C, Newell F. N. (2005) Vision and touch: independent or integrated systems for the perception of texture? *Brain Res*, 1242:59-72.
72. Olmos, A., & Kingdom, F. A. A. (2004). A biologically inspired algorithm for the recovery of shading and reflectance images. *Perception*, *33*(12), 1463–1473. https://doi.org/10.1068/p5321
73. Verrillo, R. T. (1963). Effect of Contactor Area on the Vibrotactile Threshold. *The Journal of the Acoustical Society of America*, *35*(12), 1962–1966. https://doi.org/10.1121/1.1918868